

Effective and Efficient Dropout for Deep Convolutional Neural Networks

Shaofeng Cai¹, Yao Shu¹, Wei Wang¹, Meihui Zhang², Gang Chen³, Beng Chin Ooi¹

¹ {shaofeng, shuyao95, wangwei, ooibc}@comp.nus.edu.sg, National University of Singapore

² meihui_zhang@yeah.net, Beijing Institute of Technology

³ cg@zju.edu.cn, Zhejiang University

Abstract—Machine-learning-based data-driven applications have become ubiquitous, e.g., health-care analysis and database system optimization. Big training data and large (deep) models are crucial for good performance. Dropout has been widely used as an efficient regularization technique to prevent large models from overfitting. However, many recent works show that dropout does not bring much performance improvement for deep convolutional neural networks (CNNs), a popular deep learning model for data-driven applications. In this paper, we revisit the problem and investigate its failure. We attribute the failure to the conflict between the conventional dropout and the batch normalization operation after it. We propose to adjust the order of the dropout operations to address the conflict; and further, other structurally more suited dropout variants are also examined and introduced for more efficient and effective regularization for CNNs. These dropout variants can be easily integrated into the building blocks of CNNs implemented by existing deep learning libraries, e.g., Apache Singa, to provide effective regularization for CNNs. Extensive experiments on benchmark datasets CIFAR, SVHN and ImageNet are conducted to compare the existing building blocks and the proposed building blocks with the proposed customizable dropout methods. The results confirm the superiority of our building blocks due to the regularization and implicit model ensemble effect of dropout. In particular, we improve over state-of-the-art CNNs with significantly better performance of 3.17%, 16.15%, 1.44%, 21.68% error rate on CIFAR-10, CIFAR-100, SVHN and ImageNet respectively.

I. INTRODUCTION

Recently, with big data and the proliferation of machine learning, especially deep learning, there is a surge of machine-learning-based data-driven [27] applications including deep-learning-based video stream analysis [18], health-care analysis [5] and database system optimization [25], [34]. Deep learning models are getting larger and deeper to increase the capacity for higher performance (e.g., accuracy). It is therefore not surprising that deep convolutional neural networks (CNNs) have led to a series of breakthroughs on a variety of tasks [8], [14], [21]. However, large complex models typically comprise of hundreds of layers with millions of parameters [15], [38], which are unfortunately prone to overfitting. Overfitting is indeed a fundamental challenge of machine learning.

Many explicit and implicit regularization methods have been proposed to address overfitting, including early stopping, weight decay, data augmentation etc. Dropout [11], [30] is empirically more attractive among the existing methods due to its efficiency and effectiveness. In each training iteration, the

standard dropout randomly samples a set of neurons and deactivates them, and then trains on the remaining sub-network. Consequently, different iterations are training over different sub-networks. The original full network can thus be regarded as an economic ensemble of an exponentially large number of sub-networks. In this sense, dropout has similar effects as the sampling techniques in some database and data mining algorithms. For example, in locality-sensitive hashing [7], the hash family is amplified by sampling many hash functions to create an ensemble; in the SON algorithm [28] for frequent itemset mining, the dataset is randomly sampled to run the A-Priori algorithm [1] repeatedly, whose results are aggregated together. Besides the ensemble effect, dropout also regularizes the networks by discouraging complex co-adaptation between the representation learnt by neurons and therefore contributes to more robust feature extraction.

Recent applications of dropout in convolutional neural networks [9], [15], [39] fail to obtain significant performance improvement. Initially, dropout [11], [30] is introduced to the fully connected layers [21] of neural networks. Recent CNN models replace the fully connected layers with a global average pooling layer [24]. Many CNNs have also tried to apply dropout to convolution layers. For instance, WRN [39] applies a dropout layer between two wide convolution layers of the residual block and reports noticeable improvement. However, dropout in these CNNs is still adopted at the neuron level, which turns out to be less effective. Even negative effects are observed [10] when applying dropout to the identity mapping part of the residual block in ResNet [9]. The effect of dropout in CNNs is further diminished by the introduction of other regularization techniques such as data augmentation and particularly batch normalization [17].

To better integrate dropout into CNNs, we revisit the existing dropout methods applied at different structural levels, namely neuron, channel, path and layer level. In a way reminiscent of the sampling in LSH that samples against different hash functions for different data, e.g., MinHash for word sets, we may need to sample against different structural levels for CNN models. We present a unified framework to introduce and analyze the four dropout methods, which are denoted as drop-neuron, drop-channel, drop-path and drop-layer respectively. To appreciate the reason why existing dropout methods fail when applied to convolutional layers of CNN models, we investigate the interaction between dropout and other standard

techniques or layers adopted in CNNs, mainly data augmentation and particularly batch normalization [17]. We attribute the failure of standard dropouts to the increase of variance from the random deactivation of the basic components, e.g. neurons in drop-neuron and channels in drop-channel, which conflicts with the batch normalization layer following each convolutional layer.

We therefore propose to reorder the dropout and batch normalization in the convolutional building blocks to address this problem. Further, customizable convolutional building blocks are proposed with a pipeline of common layers, including the dropout, convolution, batch normalization layer and etc, for ease of use. As validated in extensive experiments, these blocks achieve consistently better performance than existing building blocks. The advantages of the proposed building blocks and training mechanisms for deep CNNs are threefold. Firstly, all four dropout methods can be readily implemented as neural network layers or operations in existing deep learning libraries such as Apache SINGA¹ initiated by us, as illustrated in Figure 1. Second, all of these dropout methods are computationally lightweight and imposes a negligible increase in model complexity. Third, the introduction of different levels of dropouts to convolutional layers of CNNs, especially drop-channel, provides a more effective regularization. To support these claims, extensive experiments are conducted over state-of-the-art CNNs. We adopt widely benchmarked datasets CIFAR-10, CIFAR-100, SVHN and ImageNet, where significant improvement in terms of accuracy is observed even upon extensive data augmentation and batch normalization. With the proposed convolutional building blocks, state-of-the-art CNNs further improve the accuracy significantly.

The main contributions are:

- We present a unified framework for analyzing dropout methods in CNNs. Specifically, we investigate the failure of two types of dropouts, which is mainly due to their incorrect placement in the convolutional block.
- We propose convolutional building blocks that are better in line with dropout training mechanisms, which are readily applicable to existing CNN architectures.
- Extensive experiments are conducted to compare different dropout methods and validate the effectiveness of the proposed dropout blocks, with which we achieve significant improvement over state-of-the-art CNNs.

The remainder of the paper is organized as follows. Section II introduces the background. In Section III, we formulate the convolutional transformation in a unified framework, based on which training mechanisms of the four structural levels of dropouts are proposed with general convolutional building blocks for deep CNNs. Experimental evaluations of the effectiveness of our proposed convolutional building blocks are provided in Section IV. Section V concludes the paper.

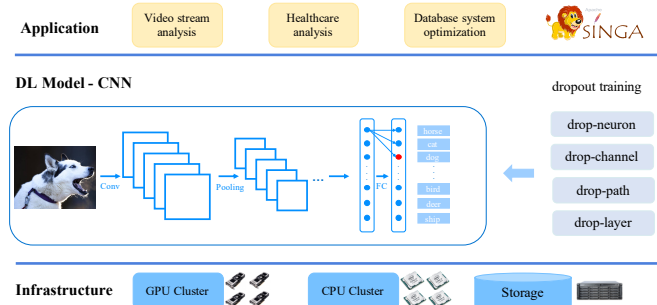


Fig. 1: Supporting complex analytics with dropout training.

II. BACKGROUND

A. Deep Convolutional Neural Networks

Convolutional neural networks (CNNs) in recent years grow deeper and wider. AlexNet [21] proposes an 8 layers CNN for image classification on ImageNet. VGG [29] and GoogLeNet [32] push the depth of CNNs to 19 and 22 respectively by stacking the basic convolutional building blocks, e.g., Inception module in GoogLeNet. ResNet [9] proposes a deep residual learning model that enables the training of much deeper CNNs over 1000 layers.

Complementarily to the depth, widening each layer can also lead to finer representation learning. [24] replaces the filter kernel of the convolutional transformation with a multilayer perceptron, which allows for complex and learnable interactions between input channels. CNNs such as Inception series [32] and ResNeXt [38] instead explore group convolution [21], using the multi-branch convolutional operation.

New building blocks of CNNs have also been proposed. For instance, the convolutional layers of NIN [24] and Inception modules [32] enable more sophisticated feature extractions. Residual building blocks with identity mapping residual connection [9], [10] supports deeper models. Dense blocks in DenseNet [15] facilitates layer-wise feature reuse by forwarding activation maps to subsequent layers.

B. Dropout for Deep Neural Networks

Regularization is essential for deep neural networks. Many regularization methods have been proposed, e.g., weight decay, data augmentation, batch normalization [17] etc. Dropout [11], [30] empirically proves to be more efficient and effective.

[35] shows that dropout performs a form of adaptive regularization for generalized linear models, which is first-order equivalent to an L_2 regularizer. Further, dropout provides immediately the magnitude of the regularization, which is adaptively scaled by the inputs and the variance of the dropout variables [2]. [6], [19] instead analyze dropout in the Bayesian inference framework for uncertainty modeling.

Many relevant implicit model ensemble techniques based on dropout have also been explored subsequently. Swapout generalizes dropout with a stochastic training method, which samples sub-network for training from either dropout, stochastic depth [16] or the residual connection [9]. DropConnect [36]

¹https://en.wikipedia.org/wiki/Apache_SINGA

instead introduces randomness to connections and randomly deactivates connections during training. Model Slicing [3] trains the model with each layer sliced with a dynamic width that starts from the first component, to support inference at different widths for runtime accuracy-efficiency trade-offs.

Different structural levels of dropout variants have also been proposed. SpatialDropout [33] shows that adding one additional layer with dropout applied to channels can improve performance in object localization. Drop-path [22] proposes to randomly drops individual paths during training and Stochastic depth [16] randomly drops a subset of layers and forwards the information with identity mapping during training. These dropout variants for CNNs apply dropout to basic components of CNNs, i.e., channel, path and layer respectively, which help regularize models for better performance.

III. DROPOUT FOR CONVOLUTIONAL NEURAL NETWORKS

In this section, we formulate the basic transformations of convolutional neural networks from the viewpoint of split-transform-aggregate. We then introduce general training mechanisms with dropout operations of different structural levels for CNNs. We also examine various architectures and propose convolutional building blocks that are better in line with the introduced dropout operations for more efficient and effective regularization.

A. The Basic Transformations of CNNs

Broadly speaking, the topology of neural networks, including multi-layer perceptron, recurrent neural networks [4], [12] and convolutional neural networks [9], [15], [21], can be represented precisely by a set of neurons and their connections, where the information flow from input neurons to output neurons is regulated by learnable weights of each connection. Succinctly, each neuron aggregates information from its input neurons:

$$y_i = \sum_{j=1}^N w_{ij} x_j \quad (1)$$

where $\mathbf{x} = [x_1, x_2, \dots, x_N]$ is a N-dimension input vector and w_{ij} the weight of the connection from input neuron x_j to the output neuron y_i . We omit output nonlinearity here for brevity. The neuron transformation follows the strategy of split-transform-aggregate, which can be interpreted as extracting features from all the input branches by first the inner product transformation of input information with corresponding weights and then an aggregation over input dimensions.

The transformation of convolutional neural networks can be formulated at a higher structural level with channels as the basic components instead of neurons. The most fundamental operation in CNNs comes from the convolutional layer which can be constructed to represent any given transformation $\mathcal{F}_{conv} : \mathbf{X} \rightarrow \mathbf{Y}$, where $\mathbf{X} \in \mathbb{R}^{C_{in} \times W_{in} \times H_{in}}$ is the input of C_{in} channels with size $W_{in} \times H_{in}$, $\mathbf{Y} \in \mathbb{R}^{C_{out} \times W_{out} \times H_{out}}$ the output likewise.

Denoting \mathbf{X}, \mathbf{Y} as $[\mathbf{x}_1, \mathbf{x}_2, \dots, \mathbf{x}_{C_{in}}]$, $[\mathbf{y}_1, \mathbf{y}_2, \dots, \mathbf{y}_{C_{out}}]$ respectively in vector of channels, the parameter set associated with each convolutional layer comprises a series of filter kernels $\mathbf{W} = [\mathbf{w}_1, \mathbf{w}_2, \dots, \mathbf{w}_{C_{out}}]$. Then the convolutional transformation on \mathbf{X} can be succinctly represented as:

$$\mathbf{y}_i = \mathbf{w}_i * \mathbf{X} = \sum_{j=1}^{C_{in}} \mathbf{w}_i^j * \mathbf{x}_j \quad (2)$$

where $*$ denotes convolution operation, and \mathbf{w}_i^j is a 2D spatial kernel associated with i_{th} output channel \mathbf{y}_i and convolves on j_{th} input channel \mathbf{x}_j . Each \mathbf{y}_i is typically followed by some output nonlinearity, which is omitted here for succinctness.

We argue that the channel level representation more natural to the convolutional transformation of CNNs. Structurally, CNNs consist of a stack of convolutional layers and for each convolutional layer, the transformation convolves over channels as in Equation 2. Unlike dense layers such as fully connected layers where each connection between input and output neurons is coupled with one learnable weight, neurons within the same channel share the same filter kernel for each output channel in CNNs. Such a weight sharing strategy dramatically reduces the number of parameters of CNNs and suggests that CNNs extract features at the channel level. This is also supported by the visualization of convolutional kernels [21], [40], where filter kernels of the data-connected layer learn to identify orientations and colored blobs and increasing invariance and class discrimination is observed ascending the layers.

B. Dropout Operations for CNNs

In this subsection, we recapitulate mainstream convolutional transformations of representative CNNs. To enhance the training of CNNs, four structural levels of dropout operations are introduced and analyzed. We then propose general convolutional building blocks designed with built-in dropout operations and training mechanisms for CNNs.

1) *Convolution Transformation Blocks*: We illustrate mainstream convolutional transformation in Figure 2. Conventional convolution transforms via operation 2 and 4, namely an identity mapping of \mathbf{X} and then a convolutional transformation \mathcal{F}_{conv} , which conforms to the formulation in Equation 2. It worth noting that group convolution [21] and depth-wise convolution [13] can also be represented under this formulation with certain constraints on the connection between channels.

Many convolutional transformations try to lengthen and/or widen the transformation. For instance, NIN [24] lengthens \mathcal{F}_{conv} by following the filter kernel with two layers of multi-layer perceptron transformation, which is structurally equivalent to two convolutional layers with 1×1 filter. Inception series [31], [32] widen \mathcal{F}_{conv} with multiple heterogeneous transformation branches. ResNeXt [38] follows similar strategy by duplicating it P times $\mathcal{F}_{conv}(\mathbf{X}) = \sum_{i=1}^P \mathcal{F}_{conv_i}(\mathbf{X})$, where the transformations are of the same topology.

Other convolutional transformations exploit feature reuse by forwarding input channels \mathbf{X} directly to output channels

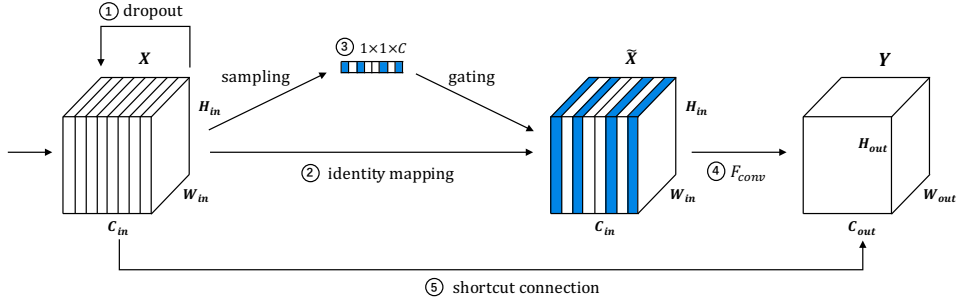


Fig. 2: Illustration of various convolutional transformations. Dropout, or drop-neuron, gates input neurons in operation 1; Drop-channel replaces identity mapping in operation 2 with operation 3, random sampling and gating on channels; Drop-path is introduced to \mathcal{F}_{conv} in operation 4 and Drop-layer to the shortcut connection in operation 5.

Y , as is indicated in operation 5. One commonly-adopted type of the feature reuse is a shortcut of identity mapping proposed in ResNet [9], [10], i.e. $Y = \mathcal{F}_{conv}(X) + X$. The shortcut structure facilitates gradient flowing back and encourages residual learning. DenseNet [15] instead proposes direct feature reuse by forwarding and appending input channels X directly to Y , specifically $\tilde{Y} = [X; Y]$.

2) *Drop-neuron - The Neuron Level Dropout*: Dropout [11], [30] empirically shows to improve the training of deep neural networks as an effective regularization and implicit model ensemble method. The standard dropout is applied to every single neuron with a single parameter p during training, controlling the participation of each neuron x_j with a gating variable α_j for each forward pass:

$$y_i = \frac{1}{p} \sum_{j=1}^N w_{ij}(\alpha_j \cdot x_j), \alpha_j \sim \text{Bernoulli}(p) \quad (3)$$

where \cdot denotes scalar multiplication and α_j is an *independent* Bernoulli random variable which takes the value 1 with probability p (the retain ratio) and the value 0 with probability $q = 1 - p$ (the drop ratio). The $\frac{1}{p}$ here scales the output activation to maintain the expected value of the output during training. Then during inference, the transformation is simply the same as in Equation 1. The standard neuron level dropout, which we name it drop-neuron to differentiate canonical dropout with other higher structural levels of dropouts, introduces randomness to the training process, which forces each neuron to learn more robust representations that are effective with different input neuron set, thus improves generalization. Therefore, the resulting network can then be regarded as the ensemble of exponentially many subnets.

The neuron level dropout empirically demonstrated to be effective for deep neural networks, especially for dense layers, as is illustrated in operation 1 of Figure 2. However, recent state-of-the-art CNN models [9], [14], [15] find that dropout is ineffective when applied to convolutional layers. We note that this is mainly because for CNNs, features are extracted channel-wise during convolutional operation, therefore the neuron level dropout can hardly improve training, whose con-

tribution is quite limited when trained together with extensive data augmentation.

3) *Drop-channel - The Channel Level Dropout*: The channel level dropout, i.e., drop-channel, is inspired by the observation that there exists a close structural correspondence between channels in convolutional layer and neurons in canonical neural networks, which is formulated formally in Equation 1, Equation 2. With similar derivation, drop-channel can be formulated as:

$$y_i = w_i * \tilde{X} = \frac{1}{p} \sum_{j=1}^{C_{in}} w_i^j * (\alpha_j \cdot x_j) \quad (4)$$

where α_j is again an *independent* Bernoulli random variable with probability $1 - p$ of being 1 and is applied to the entire channel x_j . Particularly, α_j controls the presence of channel x_j during training. The drop-channel training is illustrated in Figure 2, where the identity mapping of operation 2 is replaced by operation 3, a random sampling of α_j followed by the corresponding gating. The $\frac{1}{p}$ here again compensates for the scale loss from the deactivation of input channels and maintain the expected value of the output during training. The resulting network after training then can be directly used for inference with Equation 2.

The idea of channel level dropout is first introduced in SpatialDropout [33]. However, [33] only shows that SpatialDropout improves CNN models over an object localization dataset and the effectiveness of SpatialDropout in interaction with other training techniques, e.g., data augmentation and batch normalization [17], are not properly examined. To exploit both regularization and ensemble effects, we investigate further in the sophisticated interaction between drop-channel and these techniques extensively used in state-of-the-art CNNs.

$$\hat{x}_j = \frac{x_j - \mu_j}{\sqrt{\sigma_j^2 + \epsilon}}; x'_j = \gamma_j \hat{x}_j + \beta_j \quad (5)$$

Each convolutional layer of state-of-the-art CNN models is typically followed with a batch normalization layer (BN) [17] to normalize inputs batch-wise, which stabilizes the mean and

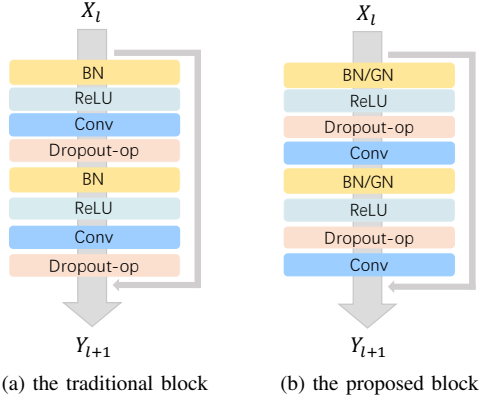


Fig. 3: The proposed convolutional building blocks with drop-operations, for both drop-channel and drop-neuron, demonstrated with the Pre-activation residual convolution block.

variance of the input channels \mathbf{X} received by each output channel \mathbf{y}_i . Take the pre-activation convolutional layers [10], [14], [15] for example, the convolutional transformation follows the *BN-ReLU-Conv* transformation pipeline, as illustrated in Figure 3a. We note that the dropout operation, including drop-neuron and drop-channel, is not incorporated into the convolutional transformation properly, which is either totally discarded in recent CNNs or used in an erroneous way. As shown in Equation 5, the BN layer normalizes each input channel \mathbf{x}_j with the batch channel mean μ_j and variance σ_j and keeps records of running estimates of them, which will be directly used for the normalization of the j th input channel after training. γ_j and β_j are learnable affine transformation parameters associated with channel \mathbf{x}_j .

However, the dropout operation is traditionally introduced right between the convolutional layer and the BN layer, which leads to violent fluctuation of the mean and variance of inputs received by the BN layer, for both drop-neuron and drop-channel. We attribute the failure of the standard dropout to the incorrect placement of the dropout operations and propose general convolutional building blocks with the dropout operation incorporated right before each convolutional layer in Figure 3b. The introduction of drop-operations before the convolutional operation, as is also analyzed in the local reparameterization of the variational dropout [19], leads to lower gradient variance and thus much faster convergence. Extensive experiments on various state-of-the-art CNNs also empirically confirm the effectiveness of the proposed convolutional building blocks in Section IV.

The disharmony between drop-neuron and the BN layer has also been theoretically analyzed in [23], which shows that there exists inconsistency of variances between the neuron level dropout and BN. The *variance shift* from training to inference leads to unstable predictions and thus possibly worse performance. We further formally show that for CNNs, the *variance shift* can be largely alleviated with drop-channel placing right before the convolutional layer. In CNNs, inputs are

normalized channel-wise and different channels transform with different kernels. Therefore, we denote that inputs from the j th channel \mathbf{x}_j share the same mean β_j and variance γ_j^2 (i.e. $E(x_{j,k}) = \beta_j$ and $\text{Var}(x_{j,k}) = \gamma_j^2$), and assume uncorrelatedness between different channels (i.e. $\text{Cov}(x_{i,\cdot}, x_{j,\cdot}) = 0$). Then for drop-channel in the traditional block, dropout operates on \mathbf{y}_i as in Equation 2 (the input \mathbf{x}_i of the next layer), and outputs $y'_{i,k} = \frac{1}{p}\alpha_i y_{i,k}$ during training. Omitting subscript i, k , we thus have:

$$\begin{aligned} \text{Var}^{Train}(y') &= \frac{1}{p^2} E(\alpha^2) E(y^2) - \frac{1}{p^2} (E(\alpha) E(y))^2 \\ &= \frac{1}{p} \gamma^2 + \frac{1-p}{p} \beta^2 \end{aligned} \quad (6)$$

The BN layer following \mathbf{y}_i keeps a record of the variance $\text{Var}^{Train}(y'_i)$ and directly uses the running estimate of it during inference. This BN estimation of variance deviates from the true variance $\text{Var}^{Test}(y') = \gamma^2$, and the shift ratio is:

$$\Delta(p)' = \frac{\text{Var}^{Train}(y')}{\text{Var}^{Test}(y')} = \frac{1}{p} + \frac{1-p}{p} \frac{\beta^2}{\gamma^2} \quad (7)$$

Therefore, there exists a variance shift of ratio $\Delta(p) \geq 1$, and $\Delta(p) = 1$ only when the channel retain ratio p is 1, i.e., no dropout operation at all. In the proposed convolutional building block, however, dropout instead operates on \mathbf{x}_i as in Equation 4 right after the convolution operation. We vectorize the kernel in the channel dimension; then for each output $y_{i,k}$ of \mathbf{y}_i , we have $y_{i,k} = \frac{1}{p} \sum_{j=1}^{C_{in}} \sum_{d=1}^D w_{i,d}^j \cdot (\alpha_j \cdot x_{j,k*d})$, where $x_{j,k*}$ denotes the vectorized receptive field of $y_{i,k}$. Omitting the subscript i, k , with uncorrelatedness we have:

$$\begin{aligned} \text{Var}^{Train}(y) &= \frac{1}{p^2} \sum_{j=1}^{C_{in}} \text{Var}[\alpha_j \sum_{d=1}^D (w_d^j x_{j,d})] \\ &= \frac{1}{p} \text{Var}^{Test}(y) + \frac{1-p}{p} \sum_{j=1}^{C_{in}} \beta_j^2 \left(\sum_{d=1}^D w_d^j \right)^2 \end{aligned} \quad (8)$$

where the inference variance is:

$$\begin{aligned} \text{Var}^{Test}(y) &= \sum_{j=1}^{C_{in}} \text{Var} \left(\sum_{d=1}^D (w_d^j x_{j,d}) \right) \\ &= \sum_{j=1}^{C_{in}} \beta_j^2 \sum_{m=1}^D \sum_{n=1}^D w_m^j w_n^j \rho_{m,n}^j \end{aligned} \quad (9)$$

where $\rho_{m,n}^j = \frac{\text{Cov}(x_{j,m}, x_{j,n})}{\sqrt{\text{Var}(x_{j,m})} \sqrt{\text{Var}(x_{j,n})}} \in [-1, 1]$. Therefore, the shift ration of the proposed drop-channel is:

$$\begin{aligned} \Delta(p) &= \frac{\text{Var}^{Train}(y)}{\text{Var}^{Test}(y)} \\ &= \frac{1}{p} + \frac{1-p}{p} \frac{\sum_{j=1}^{C_{in}} \beta_j^2 \sum_{m=1}^D \sum_{n=1}^D w_m^j w_n^j}{\sum_{j=1}^{C_{in}} \beta_j^2 \sum_{m=1}^D \sum_{n=1}^D w_m^j w_n^j \rho_{m,n}^j} \end{aligned} \quad (10)$$

We note that although $\Delta(p) \geq 1$, the variance shift of drop-channel after the convolution is smaller and more stable than $\Delta(p)'$. For $\Delta(p)'$, the β_j and γ_j^2 are the mean and variance of the activations after the convolution, which is numerically unstable during the training process and could be unbounded. For $\Delta(p)$, however, the β_j is the mean of the activations normalized by the preceding BN layer and is thus stable; the kernel weight $w_{i,d}^j$ and the covariance of between input $x_{j,m}$ and $x_{j,n}$ in the same channel \mathbf{x}_j also changes steadily as the training progresses.

Empirically, we observe less variance shift with drop-channel placed right before the convolutional layer with a relatively large retain ratio p , e.g., 0.9. Trained with drop-channel, CNNs generally improve performance considerably. We further note that the regularization and implicit model ensemble effects from drop-channel can be fully exploited by replacing BN with Group Normalization [37] (GN). GN normalizes channels within the same channel group of each layer instead of batch-wise as in BN and requires no running estimates of the channel mean and variance, and therefore leads to no variance shift.

4) Higher Level Dropout: Drop-path and Drop-layer:

Path level (drop-path) and layer level (drop-layer) dropout are proposed in FractalNet [22] and ResNet with Stochastic Depth [16] respectively. Although these two higher-level dropouts are effective in regularizing CNNs, they are highly dependent on specific CNN architectures.

Particularly, drop-path requires CNN to contain multiple paths, either homogeneous or heterogeneous, of \mathcal{F}_{conv} in operation 4 and drop-layer demands shortcut connection of operation 5 illustrated in Figure 2. Formally, drop-path can be formulated as:

$$\mathbf{Y} = \mathcal{F}_{conv}(\mathbf{X}) = \frac{1}{p} \sum_{i=1}^P \alpha_i \cdot \mathcal{F}_{conv_i}(\mathbf{X}) \quad (11)$$

where P is the number of paths (branches) of this layer, α_i is the same Bernoulli gating variable and controls the participation of i_{th} path in the transformation with the retain ratio p . In FractalNet, the drop-path is applied to the fractal architecture, where paths are heterogeneous and deviate from conventional CNN architectures. To make drop-path more applicable, we note that drop-path could be incorporated as a general building block, with the bottleneck structure [9] and group convolution [21]. Specifically, the building block is based on the bottleneck structure of one 3×3 convolution surrounded by dimensionality reducing and expanding with a 1×1 convolution, i.e., conv 1×1 -conv 3×3 -conv 1×1 . To support drop-path, the group convolution is introduced to the inner 3×3 convolutional layer with P groups as proposed by ResNeXt [38]. Then structurally, the bottleneck building block contains P independent paths of homogeneous transformations, each of which first collapses C input channels into d channels by a 1×1 convolution, and then transforms by an inner 3×3 convolution within each path and finally expands back to C channels by a 1×1 convolution. In the implemen-

tation, this building block is equivalent to the bottleneck with the inner 3×3 convolution of P groups.

We further propose to choose P to be a power of 2 empirically, e.g., 16, 32, 64 and fixed P throughout the network, and $d = \frac{C}{2P}$. During training, the building blocks trained with drop-path need to re-calibrate the activations of each path $\mathcal{F}_{conv_i}(\mathbf{X})$ by $\frac{1}{p}$ to compensate for the scale loss from the path dropout.

For the layer level dropout, we examine various architectures, e.g., randomly bypassing each convolutional layer with 1×1 shortcut transformation. However, we find out that drop-layer is better in line with the shortcut connection of identity mapping [10], [39], namely $\mathbf{Y} = \mathcal{F}_{conv}(\mathbf{X}) + \mathbf{X}$, which is already analyzed in [16]. No output scaling is needed for drop-layer since each layer learns the residual representation of a minute expected value.

5) Dropout as General Training Regularization for CNNs:

So far, we have introduced and examined the four different structural levels of dropout, i.e., drop-neuron, drop-channel, drop-path and drop-layer. The effectiveness of dropout operations mainly results from the regularization and ensemble effect [11], [30], [35], which is highly correlated with the number of basic components involved during dropout training.

We note that drop-neuron and drop-channel are readily applicable to existing CNNs with the adjustment of placing the dropout operation right before each convolutional transformation; we have also proposed the general building block in Section III-B4 that supports drop-path. Drop-layer is, however, highly dependent on the shortcut connection, which is only applicable to CNNs with residual connections [9], [38], [39].

We show that these dropout training mechanisms can be easily introduced to existing CNNs via the replacement of the original convolutional transformation with our proposed building blocks support at corresponding levels of dropout operations and share the hyper-parameter retain rate p for the desired regularization strength. Further, these four levels of dropout operation can be adopted together whenever the CNN architecture allows for it, e.g., drop-channel, drop-path and drop-layer can be adopted in ResNeXt simultaneously. Meanwhile, applying dropout incurs no additional model parameter and negligible computational cost.

IV. EXPERIMENTS

The four structural levels of dropouts are evaluated on representative CNNs on widely benchmarked datasets, including CIFAR, SVHN and ImageNet. We first introduce the dataset and training details, and CNN architectures. We then evaluate the effectiveness of the building blocks with the proposed dropout operations. We compare drop-neuron, drop-channel, drop-path and drop-layer and also their combinations, with which we improve over state-of-the-art CNNs on CIFAR and SVHN datasets and achieve consistently better results.

A. Dataset Details

1) *CIFAR*: The two CIFAR [20] datasets consist of 32×32 colored scenery images. CIFAR-10 (C10) consists of images drawn from 10 classes and CIFAR-100 (C100) from

Group	Output Size	VGG-11	WRN-16-8	ResNeXt-29-P64-d4	DenseNet-L190-K40	WRN-40-4
conv1	32×32	[conv3×3, 64]×2	[conv3×3, 16]×1	[conv3×3, 64]×1	[conv3×3, 80]×1	[conv3×3, 16]×1
conv2	32×32	-	[Block, 16×4]×6	[B-Block, 256]×4	[D-Block, 80-1320]×31	[Block, 16×8]×2
conv3	16×16	[conv3×3, 256]×2	[Block, 32×4]×6	[B-Block, 512]×4	[D-Block, 660-1900]×31	[Block, 32×8]×2
conv4	8×8	[conv3×3, 256]×2	[Block, 64×4]×6	[B-Block, 1024]×4	[D-Block, 950-2190]×31	[Block, 64×8]×2
conv5	8×8	[conv3×3, 512]×4	-	-	-	-
avgPool	1×1	[avg8×8, 512]	[avg8×8, 256]	[avg8×8, 1024]	[avg8×8, 2190]	[avg8×8, 512]
Dataset	-	CIFAR	CIFAR	CIFAR	CIFAR	SVHN
Params	-	9.89M	8.95M	8.85M	25.62M	10.96M

TABLE I: Detailed Architectures and configurations of representative convolutional neural networks for CIFAR and SVHN datasets. Building blocks are denoted as “[block, number of channels] × number of blocks”.

100 classes. The training and testing set for both datasets contain 50,000 and 10,000 images respectively. Following the standard data augmentation scheme [9], [15], [16], each image is first zero-padded with 4 pixels on each side, then randomly cropped to produce 32×32 images again, followed by a random horizontal flip. We denote the datasets with data augmentation by “+” behind the dataset names (e.g., C10+). We normalize the data using the channel means and standard deviations for data preprocessing.

2) *SVHN*: The Street View House Numbers dataset [26] contains 32×32 colors digit images from Google Street View. The task is to correctly classify the central digit into one of the 10 digit classes. The training and testing sets respectively contain 73,257 and 26,032 images, and an additional training dataset contains 531,131 images that are relatively easier to classify. We adopt a common practice [15], [16], [39] by using all the training data without any data augmentation. Following [15], [39], we divide each pixel value by 255, scaling the input to range $[0, 1]$.

3) *ImageNet*: The ILSVRC 2012 image classification dataset contains 1.2 million images for training and 50,000 for validation from 1000 classes. We adopt the same data augmentation scheme for training images following the convention [9], [15], [39], and apply a 224×224 center crop to images at test time. The results are reported on the validation set.

B. CNN Architecture Details

As discussed in Section III-B5, drop-neuron and drop-channel are generally applicable to CNNs while the applicability of drop-path and drop-layer are dependent on CNN architectures. To evaluate the effectiveness of the four levels of dropout, we therefore adopt CNN architectures with representative convolutional transformation.

Specifically, we first evaluate and compare drop-neuron and drop-channel with our proposed building blocks illustrated in Figure 3b on VGG [29], whose convolutional layer is a plain 3×3 conv following operation 2 and 4 of Figure 2. For drop-path of the new building block proposed in Section III-B4 and drop-layer, we test their effectiveness in comparison with drop-channel and drop-neuron on ResNeXt [38] with multiple paths and residual connection, Wide Residual Networks [39] (WRN) with wider convolutional layer and residual connection and DenseNet [15] with shortcut connection.

We denote these models with WRN-depth-k, ResNeXt-depth-P-d and DenseNet-L-K, with k, P, d, L, K as the widening factor [39], the number of paths, the channel width

of each path [38], the number of layers (depth) and K the growth rate [15] respectively. The building blocks of WRN, ResNeXt and DenseNet are basic block (Block) with two consecutive 3×3 conv, the bottleneck block (B-Block) proposed in III-B4 and the DenseNet bottleneck block (D-Block) [15] with dimensionality reduction of 1×1 conv and the following transformation of 3×3 conv. The detailed model configurations for CIFAR-10/100, SVHN and ImageNet datasets are provided in Table I and Table II.

For CNNs trained with drop-neuron and drop-channel, each convolutional layer is replaced with the proposed building block in Section III-B, where the dropout operations are incorporated into the transformation right before the convolution. While for drop-path, each convolutional layer is replaced with the proposed general drop-path building block in Section III-B4.

C. Training Details

For all the experiments, we train the networks with SGD and Nesterov momentum. For CIFAR datasets, we train 300 epochs on VGG-11, ResNeXt-29-P64-d4, and DenseNet-L190-K40, 200 epochs on WRN-40-4. For SVHN, we train 160 epochs on WRN-16-8. The initial learning rate is set to 0.1, weight decay 0.0001, dampening 0, momentum 0.9 and mini-batch size 128 for CIFAR and SVHN datasets. The learning rate is divided by 10 at 50% and 75% of the total number of training epochs. For ImageNet, we train 100 epochs on VGG-16, WRN-50-2, DenseNet-L169-K32 with a mini-batch size of 125. The initial learning rate is set to 0.05, and is lowered by a factor of 10 after epoch 30, 60 and 90. We use a weight decay of 0.0001 and momentum 0.9 without dampening.

D. Experimental Results

1) *Building Blocks of Drop-neuron and Drop-channel*: We validate the effectiveness of the proposed building blocks supporting drop-neuron and drop-channel on VGG-11, WRN-40-4 and DenseNet-L100-K12, as introduced in Section IV-B and Table I. The results are summarized in Table III, where we report the results of networks trained without dropout (original), with traditional drop-neuron and drop-channel (DN and DC), and with the proposed drop-neuron and drop-channel (DN+ and DC+) respectively.

We can notice that the proposed building blocks consistently improve over the original blocks by a significant margin. Comparing to the original results, networks trained with drop-neuron and drop-channel achieve significantly better

Group	Output Size	VGG-16	Output Size	WRN-50-2	DenseNet-L169-K32
conv1	224×224	[conv3×3, 64]×2	112×112	conv7×7, stride 2	conv7×7, stride 2
pooling	112×112	2×2 max pool, stride 2	56×56	3×3 max pool, stride 2	3×3 max pool, stride 2
conv2	112×112	[conv3×3, 128]×2	56×56	[B-Block, 64×2]×6	[D-Block, 64-256]×6
pooling	56×56	2×2 max pool, stride 2	28×28	conv3×3, stride 2	Transition Layer
conv3	56×56	[conv3×3, 256]×2	28×28	[B-Block, 128×2]×3	[D-Block, 128-512]×12
pooling	28×28	2×2 max pool, stride 2	14×14	conv3×3, stride 2	Transition Layer
conv4	28×28	[conv3×3, 512]×2	14×14	[B-Block, 256×2]×3	[D-Block, 256-1792]×32
pooling	14×14	2×2 max pool, stride 2	7×7	conv3×3, stride 2	Transition Layer
conv5	14×14	[conv3×3, 512]×2	7×7	[B-Block, 512×2]×3	[D-Block, 896-1920]×32
pooling	7×7	2×2 max pool, stride 2	1×1	7×7, global avg-pool	7×7, global avg-pool
FC	1000	[512×7×7,4096,4096,1000]	1000	[1024,1000]	[1920,1000]
Params	-	138.4M	-	68.9M	14.1M

TABLE II: Detailed configurations of representative CNNs for the ImageNet dataset.

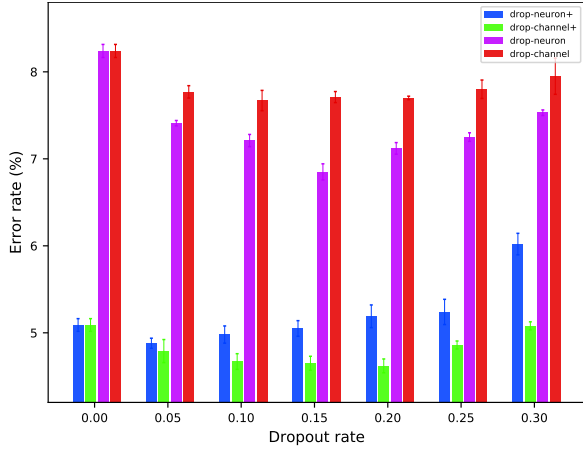


Fig. 4: Error rate (%) of VGG-11 trained with drop-neuron and drop-channel w/o data augmentation.

Network	original	DN	DN+	DC	DC+
VGG	5.09	5.18	4.98 (+0.20)	4.78	4.67 (+0.11)
WRN	4.97	4.89	4.63 (+0.26)	4.60	4.31 (+0.29)
DenseNet	4.57	4.70	4.52 (+0.18)	4.56	4.32 (+0.24)

TABLE III: Error rates (%) of Networks trained with dropout operations w/o the proposed building blocks on CIFAR-10.

performance, which demonstrates that the dropout technique is effective in regularizing CNNs if applied properly. For instance, the introduction of drop-channel alone achieves a reduction of the error rate by 0.42%, 0.66% and 0.25% on VGG-11, WRN-40-4 and DenseNet-L100-K12 respectively.

2) *Dropout operations w/o Data Augmentation*: We evaluate the relationship between data augmentation and dropout operations of drop-neuron and drop-channel for CNNs. The results are reported on VGG-11, whose error rates and learning curves are illustrated in Figure 4 and Figure 5. We denote VGG networks trained without dropout, with drop-neuron and drop-channel as VGG-11, drop-neuron and drop-channel respectively, and the network trained with standard data augmentation is marked with a suffix +.

We summarize the main results in Figure 4, where error rates and standard deviations are reported with the dropout rate searched in 0.05. The results show that data augmentation is essential for CNNs; without data augmentation, the performance decreases by around 3%. Further, drop-neuron and

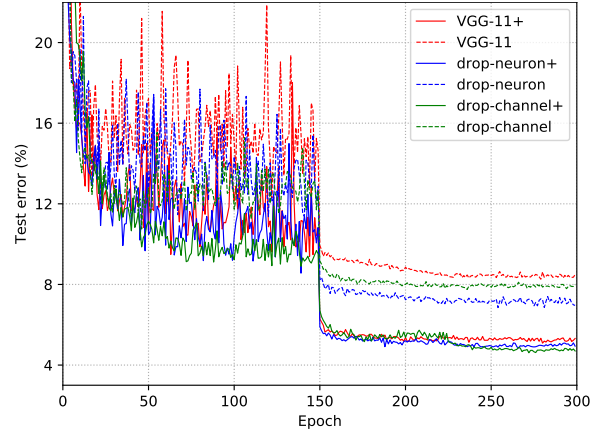


Fig. 5: Learning curves of VGG-11 trained without dropout, with drop-neuron and drop-channel w/o data augmentation.

drop-channel improve the performance both with and without data augmentation. With data augmentation and drop-channel, the model achieves the best result of 4.62% from 8.24%, i.e., 3.62% improvement; meanwhile without data augmentation, drop-neuron achieves a better result of 6.85% than drop-channel. This shows that the regularization effect of drop-neuron somewhat overlaps with data augmentation.

We further plot learning curves of networks trained with best dropout rates in Figure 5. The learning curves confirm the findings and demonstrate that drop-neuron and drop-channel are effective in regularizing CNNs. For state-of-the-art CNNs trained with extensive data augmentation, drop-channel is an effective regularization to improve the performance by a noticeable margin.

3) *The effectiveness of Drop-path*: We evaluate drop-path on ResNeXt-29-64-4 (see Table I), specifically the effect of drop-path alone and with other finer-grained dropout operations. We adopt building blocks supporting drop-path as proposed in Section III-B4.

The results of ResNeXt trained with drop-neuron, drop-channel, drop-path and dropout with both drop-path and drop-channel (drop-path-channel, with the same dropout rate from 0.05 to 0.15) are summarized in Figure 6. Results show that drop-neuron improves the performance slightly from 5.10% to 4.87%, and drop-channel outperforms drop-neuron with error rate 4.72%. With the proposed drop-path building block,

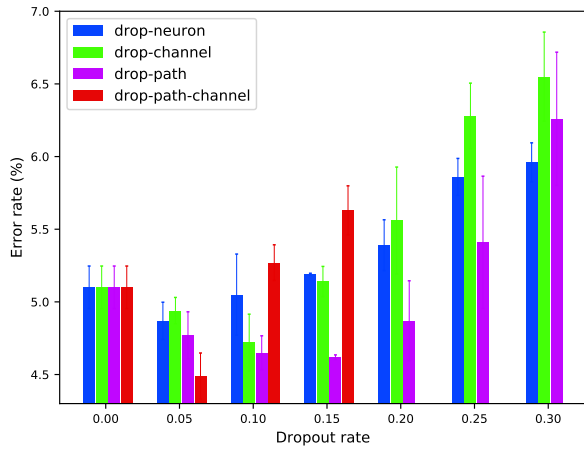


Fig. 6: Error rate (%) of ResNeXt-29-64-4 trained with drop-neuron, drop-channel and drop-path.

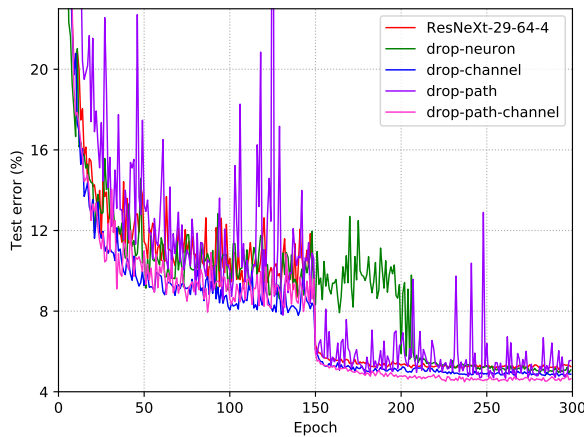


Fig. 7: Learning curves of ResNeXt-29-64-4 trained with drop-neuron, drop-channel and drop-path.

ResNeXt achieves a better result of 4.62%, i.e., 0.48% relative improvement over the network without dropout.

As discussed in Section III-B5, the path level dropout can be adopted with finer-grained drop-operations, i.e., drop-neuron and drop-channel. With both drop-channel and drop-path, ResNeXt achieves the best result of 4.49 with a dropout rate 0.05. This confirms that different levels of dropouts could possibly further improve the performance of CNNs.

To understand the impact of dropouts on the training process, we plot the learning curves trained with different dropout rates from 0.0 to 0.40 in every 0.05. The main results are summarized in Figure 8 and Figure 9. We can notice that firstly, the network trained with different dropout operations achieves noticeably better results than the network without dropout. Interestingly, the learning curve of networks with drop-path fluctuates drastically, though it achieves a better result than other dropout methods. However, when trained with drop-channel, the training is more stable and the combination yields the overall best result of 4.49% test error rate. We conjecture that this is mainly because drop-path is a more radical regularization method, where each entire path is randomly dropped, and thus has

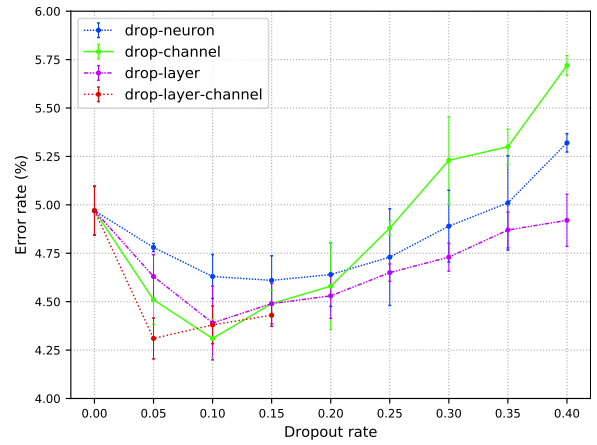


Fig. 8: Error rate (%) of WRN-40-4 trained with drop-neuron, drop-channel and drop-layer.

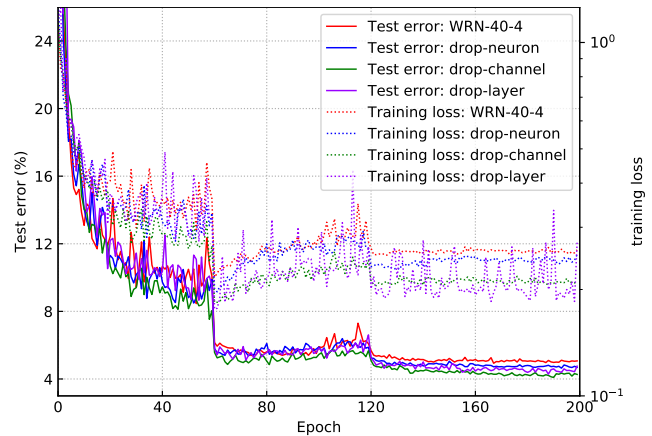


Fig. 9: Learning curves and losses of WRN-40-4 trained with drop-neuron, drop-channel and drop-layer.

higher variance. Therefore, drop-path requires a lower dropout rate.

4) *Drop-layer Revisiting*: As discussed in Section III-B4 and Section III-B5, the effect of drop-layer is examined in ResNet with Stochastic Depth [16]. To generalize drop-layer, we evaluate various design choices and find out that drop-layer is highly dependent on the residual connection with identity mapping. We further focus on comparing drop-layer with finer-grained levels of dropouts, namely drop-neuron and drop-channel. We adopt WRN-40-4 (see Table I) with dropout rate 0.05. The main results are summarized in Figure 8 and Figure 9.

We find that firstly, dropout operations help obtain noticeably better results. Further, drop-channel achieves the best result of a 0.66% reduction of test error rate from 4.97% to 4.31%. When trained with drop-channel, drop-layer improves the performance slightly, which is comparable to drop-channel alone. To appreciate the dynamics during training, we plot learning curves in Figure 9. The curves show that the training loss of the network trained with drop-layer fluctuates drastically throughout training, although the test error is rather

Model	Depth	Params	C10	C10+	C100	C100+	SVHN
VGG [29]	11	9.89M	8.24	5.09	23.58	32.08	-
↳with drop-neuron	11	9.89M	4.88	6.85	23.15	27.71	-
↳with drop-channel	11	9.89M	4.62	7.76	21.89	29.51	-
Wide ResNet [39]	40	8.95M	-	4.97	-	-	-
↳with drop-neuron	40	8.95M	-	4.61	-	-	-
↳with drop-channel	40	8.95M	-	4.31	-	-	-
↳with drop-layer	40	8.95M	-	4.39	-	-	-
Wide ResNet [39]	16	10.96M	-	-	-	-	1.54
↳with drop-neuron	16	10.96M	-	-	-	-	1.44
ResNeXt [38]	29	8.85M	-	5.10	-	-	-
↳with drop-neuron	29	8.85M	-	4.87	-	-	-
↳with drop-channel	29	8.85M	-	4.72	-	-	-
↳with drop-path	29	8.85M	-	4.62	-	-	-
DenseNet-BC (k=12) [15]	100	0.8M	5.92	4.51	24.15	22.27	1.76
↳with drop-channel	100	0.8M	5.59	4.24	23.73	20.75	1.65
DenseNet-BC (k=40) [15]	190	25.6M	-	3.46	-	17.18	-
↳with drop-neuron	190	25.6M	-	3.42	-	16.69	-
↳with drop-channel	190	25.6M	-	3.17	-	16.15	-

TABLE IV: Overall results in error rate (%) on CIFAR and SVHN datasets. A suffix + indicates standard data augmentation. Only results in the Experiments Section IV are provided for succinctness. The overall best results are **blue**.

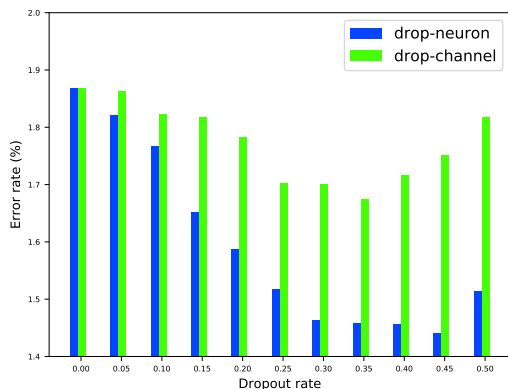


Fig. 10: Error rate (%) of WRN-16-8 trained with drop-neuron and drop-channel on SVHN.

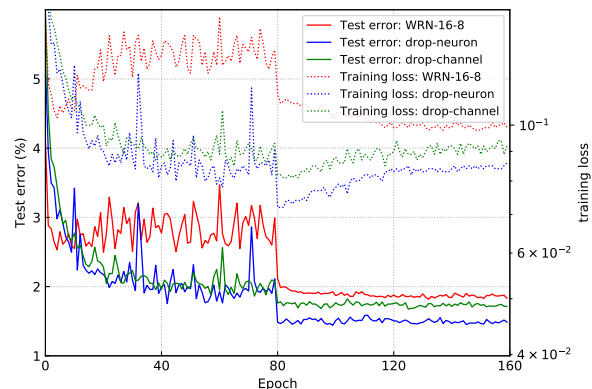


Fig. 11: Learning curves and losses of WRN-16-8 trained with drop-neuron, drop-channel on SVHN.

stable. We attribute the fluctuation to the radical reduction of basic components, i.e. layers, similar to drop-path. We therefore conclude that drop-channel is a better choice, which achieves better results with more stable training.

5) *Dropout: Better Results for State-of-the-art CNNs:* So far, we have introduced the building blocks of different levels of dropouts for improving CNNs, and meanwhile extensive experiments have been conducted on evaluating the effectiveness of different dropout operations, i.e., drop-neuron, drop-channel, drop-path and drop-layer.

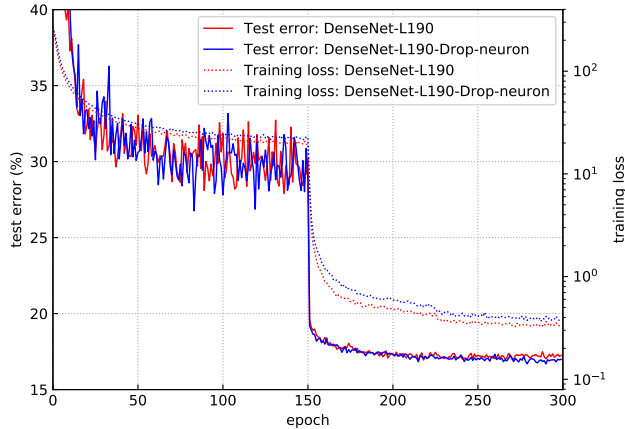
With these dropout training mechanisms introduced, we are able to further improve performance of best-performing CNNs on benchmark datasets. The overall results on CIFARs and SVHN datasets are summarized in Table IV. For SVHN, WRN-16-8 (Table I) originally achieves 1.54% error rate without data augmentation. We then introduce the proposed drop-neuron and drop-channel building blocks to WRN and the results are summarized in Figure 10 and Figure 11.

The results in Figure 10 corroborate that drop-neuron is more effective in regularizing networks trained without data augmentation. Replacing conventional convolutional layers

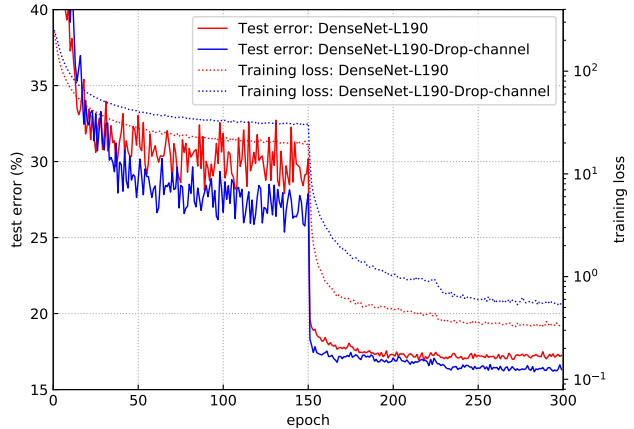
with the drop-neuron convolutional building blocks in WRN-16-8, we achieve a noticeably lower error rate of 1.44% on SVHN over the original state-of-the-art model. Figure 11 further shows that the proposed drop-neuron can effectively regularize the training process with significant lower training loss and meanwhile higher test accuracy. Without dropout regularization, the training stagnates quickly and the test error rate even increases before the first learning rate drop. While with dropouts, the training is more stable and the network continues to improve for higher accuracy.

For CIFAR datasets, the state-of-the-art model DenseNet-L190-K40 I originally achieves 4.36% and 17.18% error rates on CIFAR-10 and CIFAR-100 respectively. We then apply drop-neuron and drop-channel building blocks in replacement of convolutional layers in the model and with dropout rate 0.1, significantly better results are obtained with 3.17% and 16.15% error rates, 0.29% and 1.03% relative improvement respectively.

The overall experimental results on ImageNet dataset are summarized in Table V. Three representative CNN architectures are adopted for the large dataset, specifically VGG-



(a) CIFAR-100 w/o drop-neuron



(b) CIFAR-100 w/o drop-channel

Fig. 12: Test error and training loss curves for DenseNet-L190-K40 w/o drop-neuron and drop-channel. The two corresponding dropout rates are both set to 0.1, leading to 16.76% and 16.15% test error rate respectively on CIFAR-100+. Test error 17.18% is obtained without any dropout during training.

Model	Depth	Params	ImageNet
VGG-16 [29]	16	138.4M	27.63
↳+drop-channel	16	138.4M	27.49
WRN-50-2 [39]	50	68.9M	21.91
↳+drop-layer+channel	50	68.9M	21.68
DenseNet-L169-K32 [15]	169	14.1M	23.62
↳+drop-path+channel	169	14.1M	23.47

TABLE V: Comparison of Top-1 (single model and single crop) error rates on ImageNet classification dataset.

16 [29] with the plain convolutional operation, WRN-50-2 [39] with residual connection and DenseNet-L169-K32 [15] with a dense connection between layers. We evaluate WRN-50-2 with both drop-layer and drop-channel, and meanwhile DenseNet-L169-K32 with both drop-path and drop-channel.

For VGG-16, we improve accuracy by 0.14% with drop-channel. For WRN-50-2, we observe a more significant improvement of 0.23% with the introduction of the combination of drop-layer and drop-channel. With both drop-path and drop-channel training introduced, DenseNet-L169-K32 achieves a 0.15% test error rate reduction. The results of the three architectures on ImageNet further confirm that the dropout training mechanisms, specifically the four structural levels of dropouts alone or the combination, can significantly improve the performance if adopted properly.

Finally, to further illustrate the difference between the regularization effect of drop-neuron and drop-channel, we plot training curves of the 190 layer DenseNet on CIFAR-100+ with the two dropouts in Figure 12. The left panel indicates that the regularization effect of drop-neuron training is rather limited, which is mainly because the channel instead of the neuron is the more suited structural level to regularization for the convolutional transformation. Compared

to drop-neuron, drop-channel regularizes the model effectively and thus achieves significantly better performance. With drop-channel, the test error decreases faster and the training is more stable, especially before the first learning rate drop at epoch 150. Furthermore, DenseNet regularized by drop-channel learns with higher training loss yet with much lower test error, indicating that drop-channel prevents overfitting effectively.

V. CONCLUSION

In this paper, we examine the four structural levels of dropout training mechanisms in a unified convolutional transformation framework, including drop-neuron, drop-channel, drop-path and drop-layer. We attribute the failure of standard dropout to the incorrect placement in the convolutional building block, which incurs great training instability. Through detailed discussion and analysis, we propose general convolutional building blocks supporting different structural levels of dropouts, which are better in line with the convolutional transformation for CNNs.

Extensive analysis and experiments demonstrate that firstly, all four dropouts are effective in improving the performance of convolutional neural networks by a noticeable margin. However, among these dropout methods, drop-neuron and drop-channel are widely applicable to existing CNNs, while drop-path and drop-layer are highly dependent on the network architecture. In terms of effectiveness, drop-channel stands out from other dropouts. This is largely due to the characteristic of the convolution operation of CNNs, where the channel instead of other structural levels is the most fundamental transformation component. Therefore, drop-channel can better harness the benefits of both regularization and model ensemble. We further note that drop-channel could be more effective with

Group Normalization. Further, drop-neuron and drop-channel can be applied together with higher levels of dropouts, which can further stabilize the training process. On the other hand, drop-neuron outperforms drop-channel in the network trained without data augmentation, as is shown in Section IV-D2.

With the proposed building blocks designed with dropout training mechanisms, we achieve noticeable improvement over state-of-the-art CNNs on CIFAR-10/100, SVHN and ImageNet datasets. Given the generality and flexibility, these dropout training mechanisms would be useful for improving the performance for a wide range of deep CNNs.

REFERENCES

- [1] R. Agrawal and R. Srikant. Fast algorithms for mining association rules in large databases. In *Proceedings of the 20th International Conference on Very Large Data Bases, VLDB '94*, pages 487–499, San Francisco, CA, USA, 1994. Morgan Kaufmann Publishers Inc.
- [2] P. Baldi and P. J. Sadowski. Understanding dropout. In *Advances in Neural Information Processing Systems*, pages 2814–2822, 2013.
- [3] S. Cai, G. Chen, B. C. Ooi, and J. Gao. Model slicing for supporting complex analytics with elastic inference cost and resource constraints. *PVLDB*, 13(2):86–99, 2019.
- [4] K. Cho, B. Van Merriënboer, D. Bahdanau, and Y. Bengio. On the properties of neural machine translation: Encoder-decoder approaches. *arXiv preprint arXiv:1409.1259*, 2014.
- [5] J. Dai, M. Zhang, G. Chen, J. Fan, K. Y. Ngiam, and B. C. Ooi. Fine-grained concept linking using neural networks in healthcare. In *Proceedings of the 2018 International Conference on Management of Data*, pages 51–66. ACM, 2018.
- [6] Y. Gal and Z. Ghahramani. Dropout as a bayesian approximation: Representing model uncertainty in deep learning. In *international conference on machine learning*, pages 1050–1059, 2016.
- [7] A. Gionis, P. Indyk, and R. Motwani. Similarity search in high dimensions via hashing. In *Proceedings of the 25th International Conference on Very Large Data Bases, VLDB '99*, pages 518–529, San Francisco, CA, USA, 1999. Morgan Kaufmann Publishers Inc.
- [8] K. He, X. Zhang, S. Ren, and J. Sun. Delving deep into rectifiers: Surpassing human-level performance on imagenet classification. In *Proceedings of the IEEE international conference on computer vision*, pages 1026–1034, 2015.
- [9] K. He, X. Zhang, S. Ren, and J. Sun. Deep residual learning for image recognition. In *Proceedings of the IEEE conference on computer vision and pattern recognition*, pages 770–778, 2016.
- [10] K. He, X. Zhang, S. Ren, and J. Sun. Identity mappings in deep residual networks. In *European Conference on Computer Vision*, pages 630–645. Springer, 2016.
- [11] G. E. Hinton, N. Srivastava, A. Krizhevsky, I. Sutskever, and R. R. Salakhutdinov. Improving neural networks by preventing co-adaptation of feature detectors. *arXiv preprint arXiv:1207.0580*, 2012.
- [12] S. Hochreiter and J. Schmidhuber. Long short-term memory. *Neural computation*, 9(8):1735–1780, 1997.
- [13] A. G. Howard, M. Zhu, B. Chen, D. Kalenichenko, W. Wang, T. Weyand, M. Andreetto, and H. Adam. Mobilenets: Efficient convolutional neural networks for mobile vision applications. *arXiv preprint arXiv:1704.04861*, 2017.
- [14] J. Hu, L. Shen, and G. Sun. Squeeze-and-excitation networks. *arXiv preprint arXiv:1709.01507*, 2017.
- [15] G. Huang, Z. Liu, L. Van Der Maaten, and K. Q. Weinberger. Densely connected convolutional networks. In *Proceedings of the IEEE conference on computer vision and pattern recognition*, pages 4700–4708, 2017.
- [16] G. Huang, Y. Sun, Z. Liu, D. Sedra, and K. Q. Weinberger. Deep networks with stochastic depth. In *European Conference on Computer Vision*, pages 646–661. Springer, 2016.
- [17] S. Ioffe and C. Szegedy. Batch normalization: Accelerating deep network training by reducing internal covariate shift. In *International Conference on Machine Learning*, pages 448–456, 2015.
- [18] D. Kang, J. Emmons, F. Abuzaid, P. Bailis, and M. Zaharia. Noscope: Optimizing neural network queries over video at scale. *PVLDB*, 10(11):1586–1597, Aug. 2017.
- [19] D. P. Kingma, T. Salimans, and M. Welling. Variational dropout and the local reparameterization trick. In *Advances in Neural Information Processing Systems*, pages 2575–2583, 2015.
- [20] A. Krizhevsky and G. Hinton. Learning multiple layers of features from tiny images. *Tech Report*, 2009.
- [21] A. Krizhevsky, I. Sutskever, and G. E. Hinton. Imagenet classification with deep convolutional neural networks. In *Advances in neural information processing systems*, pages 1097–1105, 2012.
- [22] G. Larsson, M. Maire, and G. Shakhnarovich. Fractalnet: Ultra-deep neural networks without residuals. *arXiv preprint arXiv:1605.07648*, 2016.
- [23] X. Li, S. Chen, X. Hu, and J. Yang. Understanding the disharmony between dropout and batch normalization by variance shift. In *Proceedings of the IEEE Conference on Computer Vision and Pattern Recognition*, pages 2682–2690, 2019.
- [24] M. Lin, Q. Chen, and S. Yan. Network in network. *arXiv preprint arXiv:1312.4400*, 2013.
- [25] L. Ma, D. Van Aken, A. Hefny, G. Mezerhane, A. Pavlo, and G. J. Gordon. Query-based workload forecasting for self-driving database management systems. In *Proceedings of the 2018 International Conference on Management of Data*, pages 631–645. ACM, 2018.
- [26] Y. Netzer, T. Wang, A. Coates, A. Bissacco, B. Wu, and A. Y. Ng. Reading digits in natural images with unsupervised feature learning. In *NIPS workshop on deep learning and unsupervised feature learning*, volume 2011, page 5, 2011.
- [27] C. Ré, D. Agrawal, M. Balazinska, M. Cafarella, M. Jordan, T. Kraska, and R. Ramakrishnan. Machine learning and databases: The sound of things to come or a cacophony of hype? In *Proceedings of the 2015 ACM SIGMOD International Conference on Management of Data*, pages 283–284. ACM, 2015.
- [28] A. Savasere, E. Omiecinski, and S. B. Navathe. An efficient algorithm for mining association rules in large databases. In *Proceedings of the 21th International Conference on Very Large Data Bases, VLDB '95*, pages 432–444, San Francisco, CA, USA, 1995. Morgan Kaufmann Publishers Inc.
- [29] K. Simonyan and A. Zisserman. Very deep convolutional networks for large-scale image recognition. *arXiv preprint arXiv:1409.1556*, 2014.
- [30] N. Srivastava, G. E. Hinton, A. Krizhevsky, I. Sutskever, and R. Salakhutdinov. Dropout: a simple way to prevent neural networks from overfitting. *Journal of machine learning research*, 15(1):1929–1958, 2014.
- [31] C. Szegedy, S. Ioffe, V. Vanhoucke, and A. A. Alemi. Inception-v4, inception-resnet and the impact of residual connections on learning. In *AAAI*, pages 4278–4284, 2017.
- [32] C. Szegedy, W. Liu, Y. Jia, P. Sermanet, S. Reed, D. Anguelov, D. Erhan, V. Vanhoucke, and A. Rabinovich. Going deeper with convolutions. In *Proceedings of the IEEE conference on computer vision and pattern recognition*, pages 1–9, 2015.
- [33] J. Tompson, R. Goroshin, A. Jain, Y. LeCun, and C. Bregler. Efficient object localization using convolutional networks. In *Proceedings of the IEEE Conference on Computer Vision and Pattern Recognition*, pages 648–656, 2015.
- [34] D. Van Aken, A. Pavlo, G. J. Gordon, and B. Zhang. Automatic database management system tuning through large-scale machine learning. In *Proceedings of the 2017 ACM International Conference on Management of Data*, pages 1009–1024. ACM, 2017.
- [35] S. Wager, S. Wang, and P. S. Liang. Dropout training as adaptive regularization. In *Advances in neural information processing systems*, pages 351–359, 2013.
- [36] L. Wan, M. Zeiler, S. Zhang, Y. Le Cun, and R. Fergus. Regularization of neural networks using dropconnect. In *International Conference on Machine Learning*, pages 1058–1066, 2013.
- [37] Y. Wu and K. He. Group normalization. In *Proceedings of the European Conference on Computer Vision (ECCV)*, pages 3–19, 2018.
- [38] S. Xie, R. Girshick, P. Dollár, Z. Tu, and K. He. Aggregated residual transformations for deep neural networks. In *2017 IEEE Conference on Computer Vision and Pattern Recognition (CVPR)*, pages 5987–5995. IEEE, 2017.
- [39] S. Zagoruyko and N. Komodakis. Wide residual networks. *arXiv preprint arXiv:1605.07146*, 2016.
- [40] M. D. Zeiler and R. Fergus. Visualizing and understanding convolutional networks. In *European conference on computer vision*, pages 818–833. Springer, 2014.